Journal of Electroceramics, 10, 19–29, 2003

Dielectric Properties and Phase Transition Behavior of xPMN-$(1-x)$PZT Ceramic Systems

VLADIMÍR KOVAL,[1] CARLOS ALEMANY,[2] JAROSLAV BRIANČIN[1] & HELENA BRUNCKOVÁ[1]

[1] *Institute of Materials Research, SAS, Watsonova 47, 043 53 Košice, Slovak Republic*
[2] *Instituto de Ciencia de Materiales de Madrid, CSIC, Cantoblanco—280 49 Madrid, Spain*

Submitted March 7, 2002; Revised January 27, 2003; Accepted February 28, 2003

Abstract. The dielectric properties and phase transition behavior of the pseudo-ternary xPb($Mg_{1/3}Nb_{2/3}$)O_3-$(1-x)$Pb(Zr,Ti)O_3 solid solution system were investigated as a function of the Pb($Mg_{1/3}Nb_{2/3}$)O_3 (PMN) content and Ti/Zr ratio for selected compositions. The investigations have demonstrated a general trend in broadening of the phase transition and increasing diffusivity with increasing PMN content. For the morphotropic phase boundary (MPB) compositions, the dielectric permittivity maximum, its temperature (T_m) and the Curie-Weiss constant were found to decrease with increasing $Mg_{1/3}Nb_{2/3}$ concentration. When a Ti/Zr ratio was constant and equal to 53/47, temperature-dependent investigations demonstrated that the dielectric parameters involved in a modified Curie-Weiss law increase monotonically with increasing PMN content and T_m moves toward room temperature with average rate of $\approx -4.1^{\circ}$C/mol% as well. A phase transition in 0.5PMN-0.5Pb($Zr_{0.47}Ti_{0.53}$)O_3 and 0.25PMN-0.75Pb($Zr_{0.60}Ti_{0.40}$)O_3 ceramic systems exhibited a diffused behavior with a characteristic frequency dependence of T_m. From pyroelectric measurement, an unusual spontaneous polarization behavior at about 215 K is reported for some MPB compositions.

Keywords: PZT, PMN, dielectric properties, phase transitions

1. Introduction

During several past decades, many theoretical [1–3] and experimental [4–6] studies were carried out on various phase transformation and crystal structures of lead-based perovskite-type solid solutions consisting of the ferroelectric and relaxor materials. These compounds have attracted a growing fundamental and practical interest because of their excellent dielectric, piezoelectric and electrostriction properties which are useful in actuating and sensing applications [7, 8].

Experimentally it has been reported that a variety of complex-mixed perovskite relaxor ferroelectrics with a complex occupation of the A and/or B site in the crystal lattice and exhibiting the diffuse phase transition (DPT) behavior have a nanometer scale heterogeneity in composition [9, 10]. The temperature-frequency dependence of dielectric permittivity of a relaxor ferroelectric near the Curie region ($T \geq T_m$) can be described by a power relation, which was proposed by Martirena and Burfoot [11]:

$$\frac{1}{\varepsilon(\omega, T)} = \frac{1}{\varepsilon_m(\omega)}\left[1 + \frac{[T - T_m(\omega)]^{\gamma}}{2\delta_{\gamma}^2}\right], \quad (1)$$

where ω is the angular frequency, T_m is the temperature at maximum dielectric permittivity ε_m, and δ_{γ} and γ are the diffuseness parameter and critical exponent, respectively. The value of γ ($1 \leq \gamma \leq 2$) is the expression of the degree of dielectric relaxation in a relaxor.

Lead magnesium niobate, Pb($Mg_{1/3}Nb_{2/3}$)O_3 (abbreviated as PMN hereafter), is nowadays acknowledged as the representative of relaxor ferroelectrics [2]. In the PMN-type relaxor ferroelectrics either the peak of the relative dielectric permittivity or the peak of the dielectric absorption does not correlate with any macroscopic phase transition. The real macroscopic phase transition of the first order to a rhombohedral long-range ferroelectric ordered phase has been detected in PMN at about 220 K by cooling

in an external dc electric field [12]. A spontaneous (zero field) phase transition was indicated in the solid solution $Pb(Mg_{1/3}Nb_{2/3})O_3$-$PbTiO_3$ (PMN-PT) [13], $Pb(Mg_{1/3}Nb_{2/3})O_3$-$PbZrO_3$ (PMN-PZ) [4] as a result of a change in the degree of ordering induced by a substitution on cationic sites.

Ouchi et al. [14] have estabilished the phase diagram of the pseudo-ternary PMN-PZ-PT system by using the X-ray analyses and dielectric and piezoelectric measurements. Abe et al. [15] and Shilnikov et al. [16] have mentioned the compositional fluctuations and existence of polar clusters in the solid solution of PMN-PZT obtained through conventional ceramic technique.

The references on PMN-PZT, however, do not discuss a phase transition behavior of the ceramic material within an entire compositional range in detail. In addition, there have not been any studies done on the dielectric properties and the transition behavior of the solid solution between PMN and PZT prepared by a columbite method [17].

In view of the foregoing discussion, the purpose of this investigation was to study the influence of various PMN content at a specific Ti/Zr ratio on the dielectric properties and particularly the degree of phase transition diffuseness of the pseudo-ternary $(1-x)$PMN-xPZT ceramic system. As an extension of the research on the PMN-PZT perovskite system, we present here results for two series of the ceramics prepared by a columbite precursor method. The first material series represents the compositions near the MPB with $x = 0.125, 0.25$ and 0.5, and second one includes those with a Ti/Zr ratio equals to 53/47 for $x = 0.125$, 0.5 and 40/60 for $x = 0.25$. The effects of the PMN substitution into PZT on the microstructure and temperature-dependent spontaneous polarization of ceramics are discussed, too.

2. Experimental Procedure

2.1. Sample Preparation

Ceramic samples of the xPMN-$(1-x)$PZT solid solution system with the composition at the morphotropic phase boundary:

$0.125Pb(Mg_{1/3}Nb_{2/3})O_3$-$0.875Pb(Zr_{0.5}Ti_{0.5})O_3$ (abbreviated as PMN1 herafter),
$0.25Pb(Mg_{1/3}Nb_{2/3})O_3$-$0.75Pb(Zr_{0.47}Ti_{0.53})O_3$ (PMN2),
$0.5Pb(Mg_{1/3}Nb_{2/3})O_3$-$0.5Pb(Zr_{0.25}Ti_{0.75})O_3$ (PMN3)

and ceramics of the following chemical formula:
$0.125Pb(Mg_{1/3}Nb_{2/3})O_3$-$0.875Pb(Zr_{0.47}Ti_{0.53})O_3$ (PMN1T),
$0.25Pb(Mg_{1/3}Nb_{2/3})O_3$-$0.75Pb(Zr_{0.6}Ti_{0.4})O_3$ (PMN2R),
$0.5Pb(Mg_{1/3}Nb_{2/3})O_3$-$0.5Pb(Zr_{0.47}Ti_{0.53})O_3$ (PMN3P) and $Pb(Mg_{1/3}Nb_{2/3})O_3$.

were prepared in accordance with a phase diagram of PMN-PZ-PT [17] using a route based on the columbite precursor method.

The precursor of $MgNb_2O_6$ powder was synthesized from the powder oxides of $MgCO_3$ and Nb_2O_5 by calcinating of the wet-mixed mixture at 1000°C for 6 h. Next, the powders of Pb_3O_4, TiO_2, ZrO_2 and $MgNb_2O_6$ were weighed and wet-mixed according to the above chemical formula. After that, the mixture was dried, crushed and calcined at 850°C for 2 hours in an alumina crucible. The reacted material was ground and ball-milled again to fine powder, dried and pressed into disks of 13 mm in diameter and about 2 mm in thickness. The green pellets were sintered for 2 hours at 1200°C on a platinum plate covered with an alumina crucible containing a mixture of $PbZrO_3$ and ZrO_2 powders. For the properties measurement, the sintered disks were lapped step-by-step with fine-SiC papers to approximately 0.5 mm thickness, and then cleaned with methanol using an ultrasonic cleaner. The silver paste as an electrode layer was painted, and then fired on the major faces of the samples.

The samples of xPMN-$(1-x)$PZT ceramics were labeled, as given in Table 1, according to the PMN content (x) and Ti/Zr ratio. The table also summarizes the main dielectric parameters and densities of ceramic samples at room temperature.

Table 1. Composition (x), density (ρ) and dielectric parameters (ε_{RT}, tan δ) of xPMN-$(1-x)$PZT ceramics.

Sample	x	Ti/Zr	$\rho x 10^3$ (kg/m^3)	ε_{RT} (at 25°C)	tan δ (at 25°C)
PMN1	0.125	50/50	7.80	2014	0.03
PMN2	0.25	53/47	7.73	1330	0.03
PMN3	0.5	75/25	7.83	1133	0.03
PMN1T	0.125	53/47	7.86	690	0.03
PMN2R	0.25	40/60	7.79	1080	0.03
PMN3P	0.5	53/47	7.71	1440	0.03
PMN	1.0	–	7.86	5563	0.14

2.2. *Dielectric Property Measurements*

The weak-field dielectric response was measured using a low-frequency impedance analyzer HP 4192A, which can cover a frequency range from 5 Hz to 13 MHz. The samples were placed in a purpose-made furnace, which can be operated at a temperature range from room temperature to 500°C. Before the measurement, a standard calibration was performed to remove any stray capacitance, lead, and contact resistance. The temperature was measured by using a KEITHLEY 177 Microvolt DMM meter with a chromel-alumel thermocouple placed near the surface of the sample. The whole setup was controlled by a PC computer.

Temperature dependencies of the relative dielectric permittivity and dissipation factor were measured under a weak ac field (1 V_{rms}) at 8 frequencies: 0.1, 1, 10, 50, 100, 200, 500 and 1000 kHz. The temperature far from the dielectric permittivity maximum was controlled to within $\pm 1^{\circ}\text{C min}^{-1}$ using a purpose-made temperature controller. In the vicinity of dielectric permittivity peak, the dielectric measurements in cooling and heating regime were carried out at a rate of $0.5^{\circ}\text{C min}^{-1}$. The relative dielectric permittivity (ε_r) was calculated from the capacitance of the ceramic samples and their sizes.

2.3. *Pyroelectric Measurements*

The temperature dependence of the spontaneous ferroelectric polarization was measured on cooling over the temperature range 20–450°C. Low-temperature measurements were carried out on heating in a purpose-made cryostat from the temperature of LN_2 to room temperature. Thermally stimulated electric current was accumulated and the total charge was registered as a function of temperature with a programmable electrometer KEITHLEY 6512.

3. Results and Discussion

3.1. *Dielectric Properties and Compositional Effects*

Figure 1 illustrates the dielectric response recorded at 1 kHz during cooling for the samples of xPMN-$(1-x)$PZT solid solution ceramic system with the composition at the MPB. In all cases, the samples showed obvious dielectric behavior of the ferroelectrics with a DPT. As the amount of relaxor component PMN in the solid solution increases, the broadening of the dielectric permittivity versus temperature curve $\varepsilon_r(T)$ increases. The broadness in the peak dielectric permittivity curve is one of the characteristics of a ferroelectric with disordered perovskite structure. The peak relative dielectric

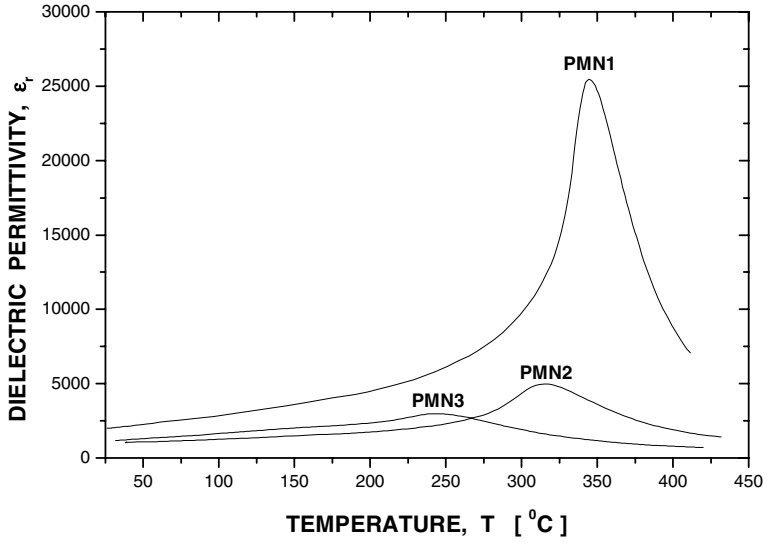

Fig. 1. Temperature dependence of the relative dielectric permittivity for xPMN-$(1-x)$PZT samples with the composition at the MPB in cooling measurement at 1 kHz.

permittivity decreases from 25500 for PMN1 to 3000 for PMN3, and the temperature for the peak dielectric permittivity decreases systematically as the content of PMN increases. These changes may be related to the distribution of ions having different ionic radii in the same sublattice of complex compound with a perovskite structure.

For a perovskite ferroelectric, it was established that the diffuseness could be caused by the decrease of grain size. Figures 2(a) and (b) give the scanning electron micrographs (TESLA BM 340) for the chemically etched

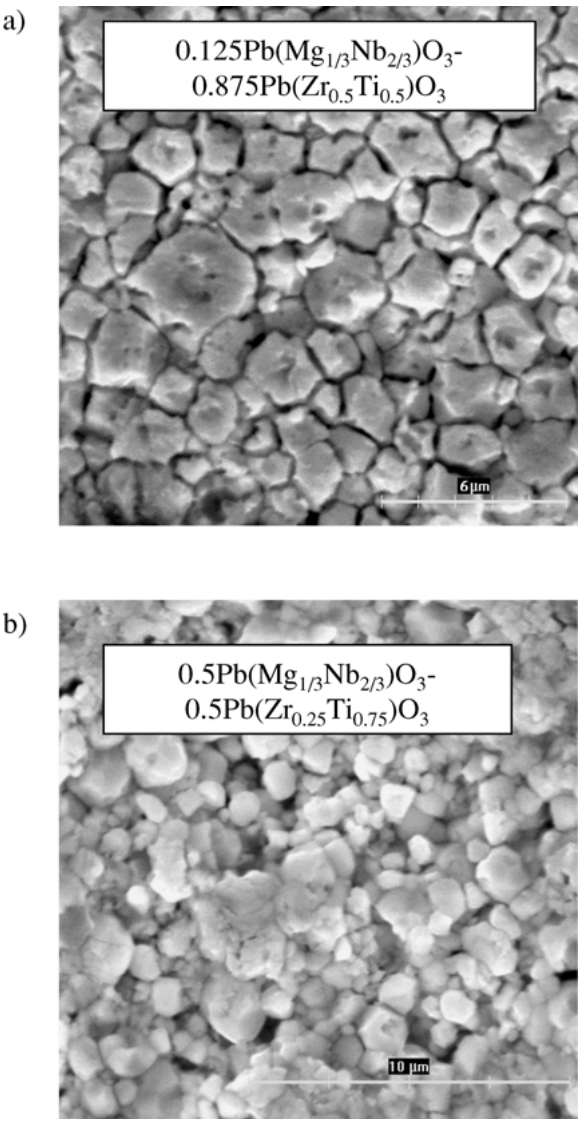

Fig. 2. SEM micrographs of xPMN-$(1-x)$PZT ceramics with the composition at the MPB. (a) $x = 0.125$ and (b) $x = 0.5$.

fractured surfaces of PMN1 and PMN3 samples, respectively. It is evident that the substitution of PMN in xPMN-$(1-x)$PZT system leads to ceramics with an average grain size of about 1 μm. However, a detailed microscopical study reveals that with increasing PMN content, the grain size does not change significantly. On the other hand, we have shown that increasing $Mg_{1/3}Nb_{2/3}$ content leads to more diffuseness of the phase transition. Thus the observed DPT behavior of xPMN-$(1-x)$PZT ceramics does not seem to be due to the grain size effect alone.

Figures 3(a) and (b) show the dielectric permittivity and loss tangent of the MPB composition samples as a function of temperature at different frequencies. It should be noted that for PMN1 ceramics ($x = 0.125$), as can be seen in Fig. 3(a), ε_r decreases with the frequency at the transition point and has two maxima at 1000 kHz. This corresponds to the fact, that a long-range ordered ferroelectric contains dipoles with the same "single" relaxation time (a relaxation frequency, $f_r \approx 10^6$ Hz near T_m). At room temperature, the dissipation factor ($\tan\delta$) is of the same order for all samples while near the transition temperature region the value increases with increasing frequency. The observed behavior follows a classical Debye-type dispersion. The slight frequency dispersion in the vicinity of the dielectric permittivity maximum is probably due to domain wall dynamics. Although the absolute values of ε_r change with frequency, the transition temperature is not shifted as for relaxors but rather remains unaffected on increasing the measurement frequency. An interesting behavior of the loss tangent in the temperature region below the dielectric permittivity maximum can be seen in Fig. 3(b) for the composition of morphotropic transformation of PMN3. With decreasing temperature, the loss tangent is nearly independent of the temperature and its value is higher than that above the critical temperature. It demonstrates a typical dielectric loss tangent behavior of a relaxor ferroelectric.

The temperature dependence of the reciprocal dielectric permittivity in paraelectric state for the MPB compositions of the xPMN-$(1-x)$PZT system followed well-known Curie-Weiss law, deviating only at temperatures close to the Curie temperature. The values of the Curie-Weiss constant (C_w), as calculated from the slope of the plot of reciprocal dielectric permittivity versus temperature in the linear part of the curve, are summarized in Table 2. As an amount of PMN and frequency increase, the value of C_w constant shows a decreasing tendency. However, it becomes

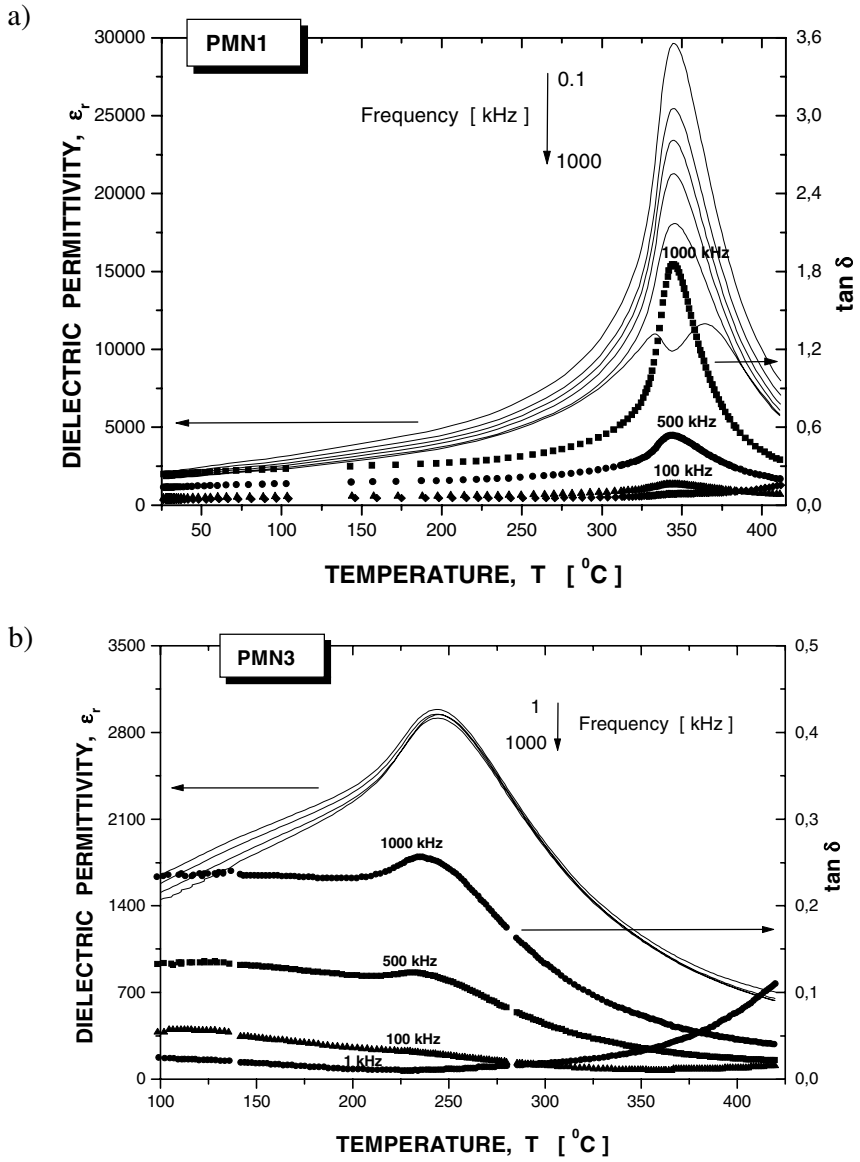

Fig. 3. Temperature dependence of the relative dielectric permittivity and dissipation factor for (a) $0.125Pb(Mg_{1/3}Nb_{2/3})O_3$-$0.875Pb(Zr_{0.5}Ti_{0.5})O_3$ (PMN1) and (b) $0.5Pb(Mg_{1/3}Nb_{2/3})O_3$-$0.5Pb(Zr_{0.25}Ti_{0.75})O_3$ (PMN3) measured on cooling at different frequencies.

almost frequency independent above $\sim 10^5$ Hz and equals to 4.0×10^5°C for PMN1, 1.4×10^5°C for PMN2 and 1.0×10^5°C for PMN3.

Considering a modified Curie-Weiss law (Eq. (1)) for the ceramics with composition at the MPB, the dependence of $\ln[(\varepsilon_m/\varepsilon_r) - 1]$ plotted against $\ln(T - T_m)$ provided the value of the diffuseness exponent γ and $\ln(2\delta_\gamma^2)$ as a slope and y-axis intercept, respectively. The calculated values of γ and δ_γ together with the values of T_m and ε_m are listed in Table 2. Since the Curie-Weiss behavior is considered as a signature of the onset of long-range order, the higher values of γ and δ_γ may originate from the decrease of the long-range correlation. In general, the values of γ and δ_γ increase nearly linearly with increasing frequency.

Figure 4 shows the variation of the relative dielectric permittivity and loss tangent measured at 1 kHz as a function of temperature on cooling for

Table 2. Various dielectric parameters involved in the Curie-Weiss law and modified Curie-Weiss law for the xPMN-$(1-x)$PZT ceramic samples at various frequencies.

Sample	$f\ x10^3$ (Hz)	T_m(°C)	ε_m	$C_w\ x10^5$ (°C^{-1})	γ	δ_γ(°C)
PMN1	0.1	344.5	29631	5.1	1.7	16.0
	1	344.4	25457	4.6	1.7	16.2
	10	344.3	23422	4.2	1.7	15.7
	100	345.2	21270	4.0	1.7	15.7
	500	345.1	18067	3.9	1.7	18.5
	1000	345.0	11632	4.0	1.7	18.0
PMN2	0.1	324.1	4933	1.9	1.6	20.3
	1	320.7	4544	1.6	1.6	20.7
	10	319.7	4331	1.5	1.7	25.1
	100	320.0	4214	1.4	1.7	25.2
	500	320.1	4115	1.4	1.7	27.6
	1000	321.4	4182	1.4	1.8	28.4
PMN3	0.1	244.7	3052	1.6	1.4	14.7
	1	243.3	2985	1.2	1.5	20.0
	10	244.5	2947	1.1	1.6	22.3
	100	244.3	2915	1.0	1.6	24.1
	500	245.5	2942	1.0	1.6	23.7
	1000	245.4	3086	1.0	1.6	25.2
PMN1T	0.1	355.1	6052	2.1	1.5	17.7
	1	355.4	5416	1.7	1.5	17.6
	10	353.3	5119	1.6	1.5	18.7
	100	353.8	4954	1.5	1.6	23.2
	500	354.2	4869	1.5	1.7	25.2
	1000	354.4	4963	1.5	1.7	25.4
PMN2R	0.1	262.1	12329	3.1	1.9	32.7
	1	262.5	11827	2.9	1.9	35.7
	10	262.9	11559	2.8	1.9	39.1
	100	263.5	10946	2.8	1.9	39.3
	500	267.6	9064	2.6	2.0	40.6
	1000	271.3	7798	2.6	2.0	47.6
PMN3P	0.1	212.9	6699	2.2	1.9	36.3
	1	212.5	6546	2.2	1.9	37.9
	10	213.1	6419	2.1	1.9	37.3
	100	215.2	6042	2.0	1.9	38.5
	500	218.1	5398	1.9	1.9	42.9
	1000	221.9	5127	1.8	1.9	45.4

f, measurement frequency, T_m, temperature of dielectric permittivity maximum, C_w, Curie-Weiss constant, ε_m, maximum relative permittivity, γ, critical exponent, δ_γ, diffuseness parameter.

the samples of xPMN-$(1-x)$PZT when a Ti/Zr ratio is constant and equals to 53/47. First, it is clear from Figs. 1 and 4 or from the plot of T_m and ε_m vs. Ti/Zr ratio on Fig. 5 that after increasing the Ti/Zr ratio in ceramic system with $x = 0.125$, the temperature of phase transition is moved to high temperature and the dielectric permittivity maximum and room-temperature dielectric permittivity are all decreased. The ferroelectric phase transition becomes more diffused without a frequency dependency of the Curie temperature.

By comparing the dielectric response of PMN2 and PMN2R illustrated in Figs. 4 and 6, respectively, one can see similar trends in behavior of T_m, ε_m and ε_{RT} with the variation of Ti/Zr ratio from 40/60 to 53/47 as those in 0.125PMN-0.875PZT system (see also Fig. 5). However, a considerable broadening of $\varepsilon_r(T)$ can be seen in Fig. 6(a) for PMN2R. Furthermore, the frequency dependence of T_m ascribed to the dynamics of polar nanodomains is present. The peaks in the values of ε_r and dielectric losses (ε'') both move towards a higher temperature as the frequency is increased, a further feature of relaxor behavior. Here, we can immediately recognize that the PMN2R sample is in a relaxor state.

By comparing the dielectric behavior of both PMN3 and PMN3P samples in Fig. 3(b) and Fig. 6(b), respectively, it is clear that PMN3P showed pronounced relaxor ferroelectric behavior characterized by a strongly diffuse dielectric peak, and a shift of the dielectric permittivity maximum to a higher temperature with increasing measurement frequency. Increasing of the Ti/Zr ratio in this system favors the ferroelectric state and retards the transition to relaxor state. This resulted in the movement of T_m to higher temperature.

Since PMN has a high dielectric permittivity of 5600 at room temperature (see ε_{RT} in Table 1), the relative dielectric permittivity of PZT is expected to increase with the addition of $Mg_{1/3}Nb_{2/3}$. In fact, Fig. 4 revealed that both ε_m and ε_{RT} increased monotonically with increasing PMN content when the Ti/Zr ratio was constant in PMN-PZT system. In addition, it can be interpreted that the temperature of dielectric permittivity peak at 0.1, 1, 10, 100, 500 and 1000 kHz moves toward room temperature almost linearly with the average rate of $\cong -4.1$°C/mol% as the molar fraction of PMN in the composition increases.

First order-like dielectric anomalies accompanied by strong thermal hysteresis effects near the peak temperature range, as shown in Fig. 7, were observed in particular for lower PMN-content samples. The dielectric response on heating underwent a maximum at a temperature ∼5°C higher than that in the cooling mode. The thermal hysteresis effects disappeared in the dielectric response of PMN2R and PMN3P, as relaxor characteristics became more evident.

The diffuseness in samples with a fixed Ti/Zr ratio (Ti/Zr = 53/47) and in PMN2R ceramics has been again determined from the plot of reciprocal dielectric

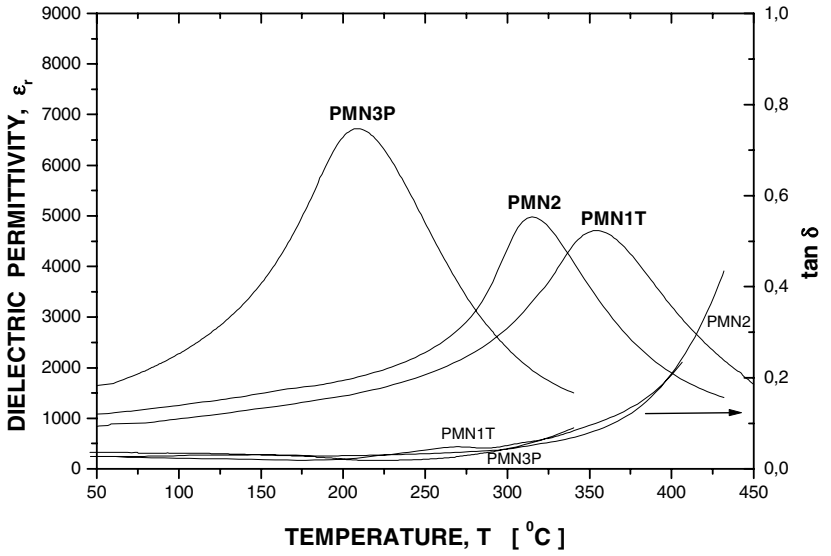

Fig. 4. Temperature dependence of the relative dielectric permittivity and dissipation factor for xPMN-$(1-x)$PZT samples with a Ti/Zr ratio of 53/47 at 1 kHz in cooling measurement.

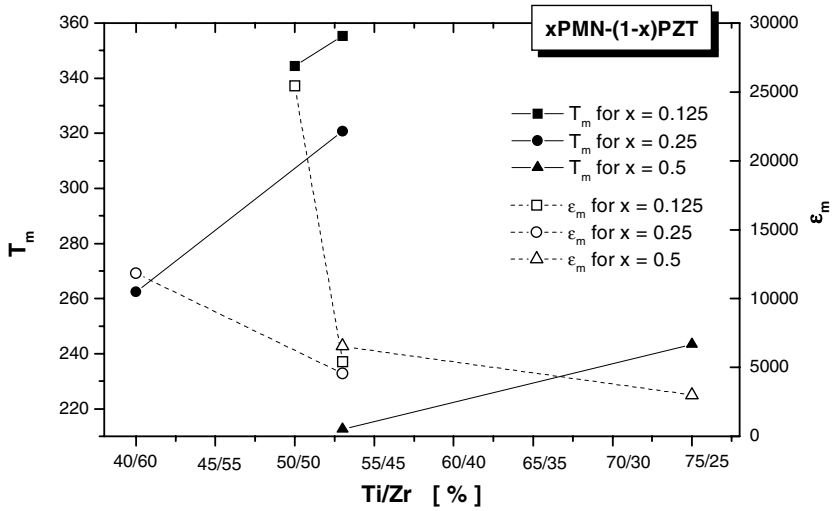

Fig. 5. Dependence of the dielectric permittivity maximum and its temperature as a function of a Ti/Zr ratio for xPMN-$(1-x)$PZT ceramics.

permittivity versus temperature. The estimated values of C_w above the Curie point are collected in Table 2. For the sample with a low $Mg_{1/3}Nb_{2/3}$ content ($x = 0.125$), the dielectric behavior in the paraelectric state fairly well obeyed the Curie-Weiss law and C_w decreased with increasing frequency. Relaxor characteristic features were observed for PMN2R and PMN3P and the Curie-Weiss behavior was found only for temperatures far above T_m. The dependencies of $\ln[(\varepsilon_m/\varepsilon_r)-1]$ vs. $\ln(T - T_m)$ exhibited similar behavior, hence data for PMN3P sample are shown as representative for 4 frequencies in Fig. 8. The estimated values of γ and δ_γ are collected in the second part of Table 2. It can be seen, that the increasing of the PMN content in xPMN-$(1-x)$PZT ceramics with Ti/Zr = 53/47 as well as the Ti/Zr ratio rise in the system with $x = 0.25$ lead to the broadening of dielectric peak and the increasing of diffusivity represented by the values of δ_γ and γ, respectively. The value of γ increases from 1.5 at $x = 0.125$ (PMN1T) to 1.9 at $x = 0.5$ (PMN3P) and thus a change

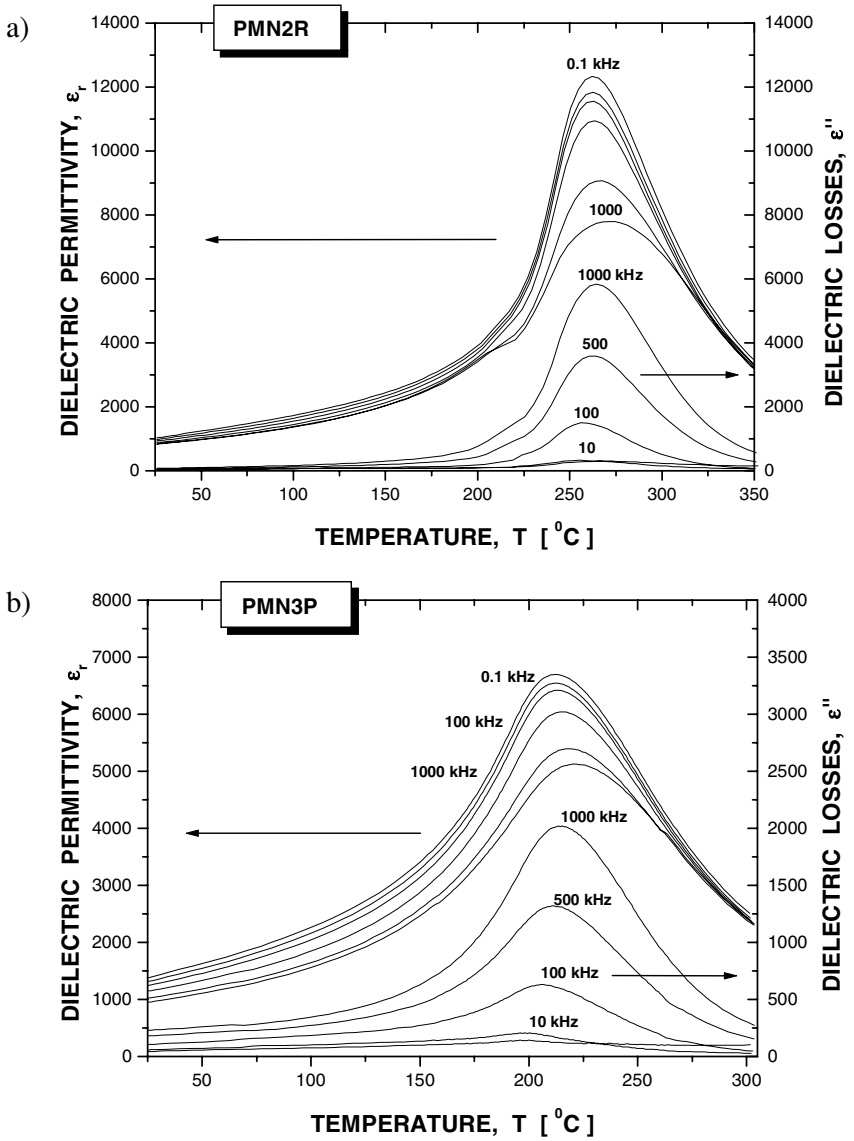

Fig. 6. Temperature dependence of the relative dielectric permittivity and dielectric losses for (a) $0.25Pb(Mg_{1/3}Nb_{2/3})O_3$-$0.75Pb(Zr_{0.6}Ti_{0.4})O_3$ (PMN2R) and (b) $0.5Pb(Mg_{1/3}Nb_{2/3})O_3$-$0.5Pb(Zr_{0.47}Ti_{0.53})O_3$ (PMN3P) measured on heating at different frequencies.

from a Curie-Weiss behavior to a modified Curie-Weiss behavior (Eq. (1)) can be observed.

3.2. Spontaneous Ferroelectric Polarization and Compositional Effects

Figure 9 presents the behavior of the spontaneous polarization P_s as a function of temperature for the xPMN-$(1-x)$PZT solid solution ceramic system from room temperature up to the paraelectric phase. The character of the phase transition as expected and deduced from dielectric measurements is of the diffused type, independently of the PMN content (x). Generally speaking, P_s decreased as x increased. An increasing of Ti/Zr ratio in the system with $x = 0.125$ and 0.25 leads to decreasing of P_s at the room temperature. On the contrary, the ceramic system with $x = 0.5$ showed a

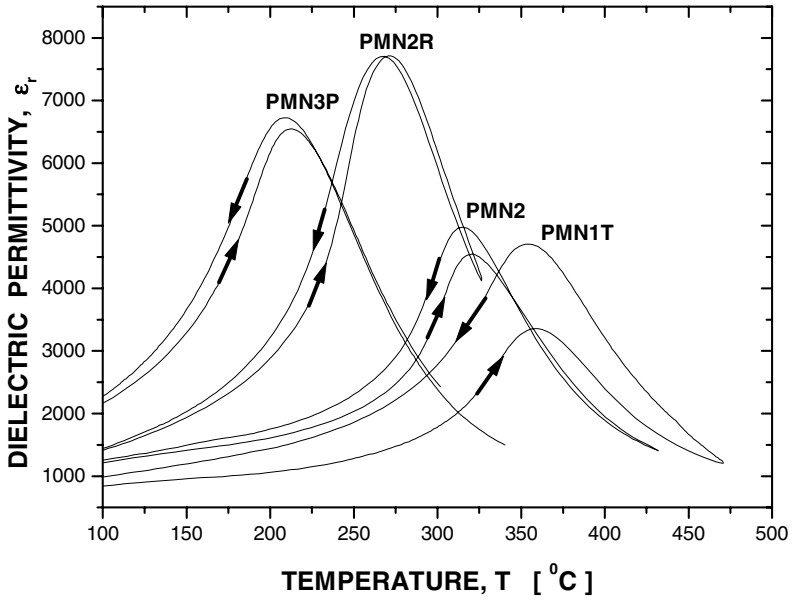

Fig. 7. Temperature dependence of the relative dielectric permittivity for 0.25Pb($Mg_{1/3}Nb_{2/3}$)O_3-0.75Pb($Zr_{0.6}Ti_{0.4}$)O_3 (PMN2R) and xPMN-$(1-x)$PZT samples with a Ti/Zr equals to 53/47 at 1 kHz in heating and cooling measurements (↑ heating, ↓ cooling).

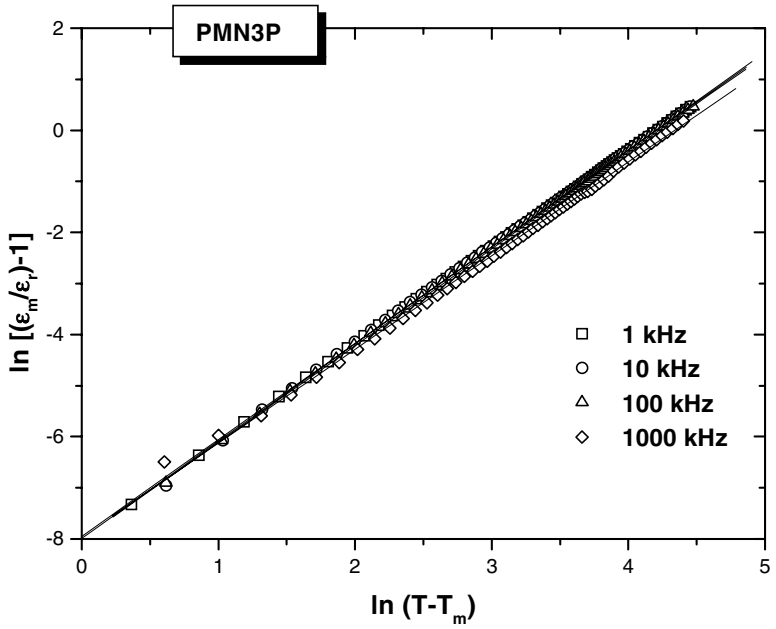

Fig. 8. Plot of $\ln[(\varepsilon_m/\varepsilon_r)-1]$ against $\ln(T-T_m)$ for the sample of 0.5Pb($Mg_{1/3}Nb_{2/3}$)O_3-0.5Pb($Zr_{0.47}Ti_{0.53}$)O_3 (PMN3P) at four frequencies. Solid lines are fits obtained from Eq. (1).

lower spontaneous polarization for a lower Ti/Zr ratio in the whole investigated temperature region. The highest spontaneous polarization $P_s = 34\ \mu C/cm^2$ is found for the MPB composition PMN1.

In order to study low-temperature polarization behavior, we measured $P_s(T)$ for selected MPB compositions of the pseudo-ternary PMN-PZT system below the room temperature up to the temperature of LN_2. The

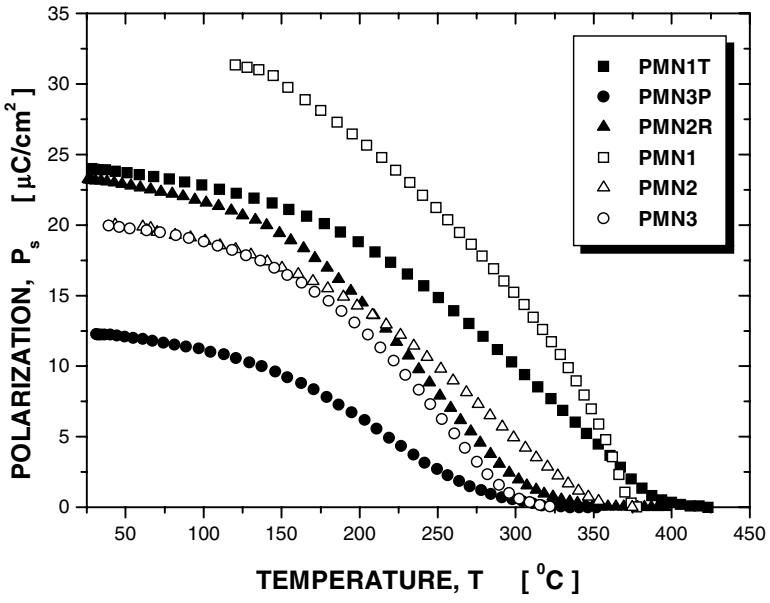

Fig. 9. Temperature dependence of the spontaneous polarization for the ceramic samples of *x*PMN-PZT solid solution system.

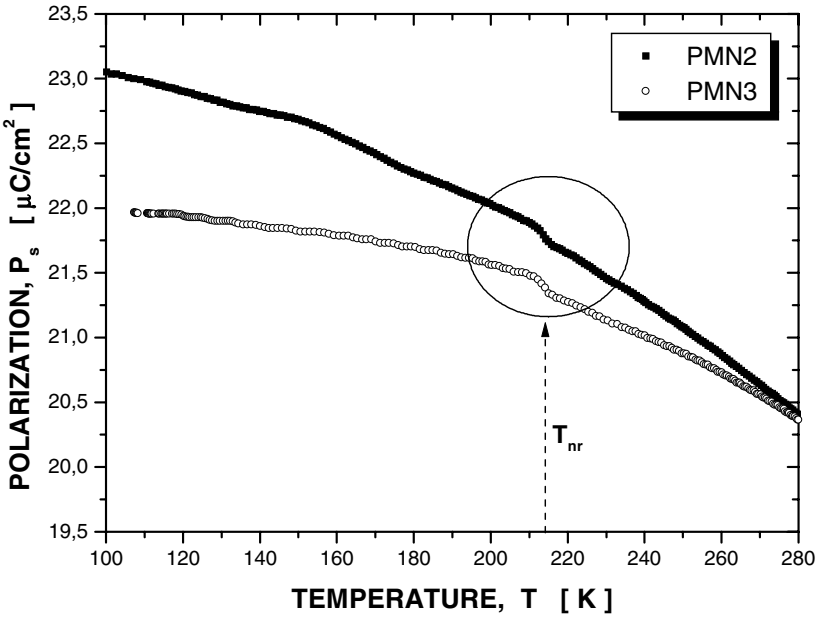

Fig. 10. Spontaneous polarization behavior of $0.5Pb(Zr_{0.25}Ti_{0.75})O_3$-$0.75Pb(Zr_{0.47}Ti_{0.53})O_3$ (PMN2) and $0.5Pb(Mg_{1/3}Nb_{2/3})O_3$-$0.5Pb(Zr_{0.25}Ti_{0.75})O_3$ (PMN3) samples in selected temperature region.

most interesting anomaly is observed for PMN2 and PMN3 at about 215 K. Inspection of Fig. 10 will reveal that with increasing temperature an evident jump in the spontaneous ferroelectric polarization appears near this temperature, indicated in Fig. 10 as T_{nr}. Since the phase transition from a short-range-ordered relaxor state to a normal ferroelectric state occurs in pure PMN with a bias field just at 217 K [12], one could deduce from the

previous results and referenced data for the PMN-PT and PMN-PZ perovskite systems that a zero-field spontaneous transition from a relaxor-like to a ferroelectric state of PMN2 and PMN3 is placed at about 215 K. The effect of a zero-field phase transformation, which is forced by a ferroelectric PZT, is believed to make the material to have a stronger ferroelectric coupling between ferroelectrically active BO_6 octahedrons and an extra polarization is obtained.

4. Conclusions

Ceramic samples of the pseudo-ternary xPb($Mg_{1/3}Nb_{2/3}$)O_3-$(1-x)$PZT solid solution system were prepared by a columbite method and investigated as a function of the PMN content and Ti/Zr ratio from the viewpoint of dielectric properties and phase transition behavior.

Based on experimental data, the following conclusions have been reached:

(1) By moving thorough the MPB to the composition with a higher PMN content ($x = 0.5$), the dielectric permittivity peak $\varepsilon_m(T)$ is found to become broadened and symmetrical without frequency dependency. Below the ε_m, relaxor-like characteristics of long-range ordered ferroelectrics were observed. An anomaly in the spontaneous polarization resembling a zero field spontaneous phase transition was detected in the MPB composition system with $x = 0.25$ and 0.5 at 215 K.

(2) From temperature-frequency-dependent data of xPMN-$(1-x)$PZT compositional series with a Ti/Zr ratio of 53/47 it was revealed that with increasing PMN content the values of ε_m, ε_{RT} and the broadness of dielectric response increase. The dependence of T_m on PMN content was nearly linear with a slope of ≈ -4.1°C/mol%. The diffuseness exponent (γ) increased as the PMN content in the system has been increased. Relaxor features were observed for the compositions of 0.25Pb($Mg_{1/3}Nb_{2/3}$)O_3-0.75Pb($Zr_{0.6}Ti_{0.4}$)O_3 and 0.5 Pb($Mg_{1/3}Nb_{2/3}$)O_3-0.5Pb($Zr_{0.47}Ti_{0.53}$)O_3.

Acknowledgments

This research was supported by the Grant Agency of the Slovak Academy of Sciences through grant No. 2/6098/99.

References

1. H. Lin, D.C. van Aken, and W. Huebner, *J. Am. Ceram. Soc.*, **82**, 2698 (1999).
2. L. E. Cross, *Ferroelectrics*, **76**, 241 (1987).
3. R. Pirc and R. Blinc, *Phys. Rev. B*, **60**, 13470 (1999).
4. K. Fan, L. Kong, L. Zhang, and X. Yao, *J. Mat. Sc.*, **34**, 6143 (1999).
5. K. Uchino, *Solid State Ionics*, **108**, 43 (1998).
6. Y. Chen, S. Hirose, D. Viehland, S. Takahashi, and K. Uchino, *Jpn. J. Appl. Phys.*, **39**, Part 1, No. 8, 4843 (2000).
7. X. Zhu and Z. Meng, *J. Mat. Sc.*, **31**, 2171 (1996).
8. K.V. Im and W.K. Choo, *Jpn. J. Appl. Phys.*, **36**, Part 1, No. 9B, 5989 (1997).
9. K. Fujishiro, T. Iwase, Y. Uesu, Y. Yamada, B. Dkhil, J. Kiat, S. Mori, and N. Yamamoto, *J. Phys. Soc. Japan*, **69**, 2331 (2000).
10. Z. Xu, S.M. Gupta, and D. Viehland, *J. Am. Ceram. Soc.*, **83**, 181 (2000).
11. H.T. Martirena and J.C. Burfoot, *Ferroelectrics*, **7**, 151 (1974).
12. A. Levstik, Z. Kutnjak, C. Filipič, and R. Pirc, *Phys. Rev. B*, **57**, 11204 (1998).
13. M. Yokosuka, *Jpn. J. Appl. Phys.*, **37**, Part 1, No. 9B, 5257 (1998).
14. H. Ouchi, K. Nagano, and S. Hayakawa, *J. Am. Ceram. Soc.*, **48**, T26 (1965).
15. Y. Abe, K. Kakegawa, and Y. Sasaki, *Nippon Kagaku Kaishi*, **10**, 671 (1999).
16. A.V. Shilnikov, A.V. Sopit, A.I. Burkhanov, and A.G. Luchaninov, *J. European Cer. Soc.*, **19**, 1295 (1999).
17. S.L. Swartz and T.R. Shrout, *Mat. Res. Bull.*, **17**, 1245 (1982).
18. N. Cereceda, B. Noheda, and J.A. Gonzalo, *J. European Cer. Soc.*, **19**, 1201 (1999).